

Composition of trapped particles in SAA

Vladimir V.Mikhailov[¶], O. Adriani^{*}, G.C. Barbarino[†], G.A. Bazilevskaya[‡], R. Bellotti[§], M. Boezio^{**},
 E.A. Bogomolov^{||}, L. Bonechi^{*}, M. Bongi^{*}, V. Bonvicini^{**}, S. Bottai^{*}, A. Bruno[§],
 F. Cafagna[§], D. Campana[†], P. Carlson^{††}, M. Casolino^{‡‡}, G. Castellini^x, M. P.De. Pascale^{‡‡},
 V. Di Felice^{‡‡}, A.M. Galper[¶], L.A. Grishantseva[¶], P. Hofverberg^{††}, A.A. Leonov[¶],
 S.V. Koldashov[¶], S.Yu. Krutkov^{||}, A.N. Kvashnin[‡], V.V. Malakhov^{**}, V. Malvezzi^{‡‡}, L. Marcelli^{‡‡},
 W. Menn^{xi}, E. Mocchiutti^{**}, S. Orsi^{††}, G. Osteria[†], P. Papini^{*}, M. Pearce^{lxix}, P. Picozza^{‡‡},
 M. Ricci^{xii}, S.B. Ricciarini^{*}, M. Simon^{xi}, N. De Simone^{‡‡}, R. Sparvoli^{‡‡}, P. Spillantini^{*},
 Yu.I. Stozhkov[‡], A. Vacchi^{**}, E. Vannuccini^{*}, G.V. Vasiliev^{||}, S.A. Voronov[¶], Y.T. Yurkin[¶],
 G. Zampa^{**}, N. Zampa^{**}, V.G. Zverev[¶]

[¶]Moscow Engineering and Physics Institute, RU-11540 Moscow, Russia

^{*} INFN, Sezione di Florence and Physics Department of University of Florence, I-50019 Sesto Fiorentino, Florence, Italy

[†]INFN, Sezione di Naples and Physics Department of University of Naples "Federico II", I-80126 Naples, Italy

[‡]Lebedev Physical Institute, Leninsky Prospekt 53, RU-119991 Moscow, Russia

[§]INFN, Sezione di Bari Physics and Department of University of Bari, I-70126 Bari, Italy

^{**}INFN, Sezione di Trieste, I-34012 Trieste, Italy

^{||}Ioffe Physical Technical Institute, RU-194021 St. Petersburg, Russia

^{††}Physics Department of the Royal Institute of Technology (KTH), SE-10691 Stockholm, Sweden

^{‡‡}INFN, Sezione di Rome "Tor Vergata" and Physics Department of University of Rome "Tor Vergata", I-00133 Rome, Italy

^xIFAC, I-50019 Sesto Fiorentino, Florence, Italy

^{xi}Physics Department of Universitaet Siegen, D-57068 Siegen, Germany

^{xii}INFN, Laboratori Nazionali di Frascati, I-Via Enrico Fermi 40, I-00044 Frascati, Italy

Abstract. The experiment PAMELA on board satellite Resurs DK1 was launched in July 2006. The instrument consists of magnetic spectrometer, imaging calorimeter, time of flight system, anticounters and neutron detector and has capability to separate electrons, positrons, protons, antiprotons and light nuclei in wide energy range from 100 MeV/n. The paper describes observations of particles composition in South Atlantic Anomaly where the satellite orbit crosses a boundary of the inner radiation belt.

Keywords: magnetosphere, radiation belt

I. INTRODUCTION

The radiation belt consists mainly of geomagnetically trapped protons, but also ions and electrons. There are several models of the radiation belts which describe protons (AP-8), electrons (AE-8), low energy ion fluxes. Recent SAMPEX and NINA-1,2 missions showed that spectra of light isotopes extend up to some tens MeV [1], [2]. Selesnick and Mewaldt [3] showed that interactions of trapped protons with atmospheric He and O can produce trapped fluxes like ²H and ³He similar to those observed. Drift averaged composition and densities from dynamic atmosphere model MSIS-90 were used in [4] to calculate secondary nuclei source functions. New attempts were made recently to improve proton and secondary production models using modern knowledge about atmosphere composition, galactic cosmic rays,

solar cosmic rays, geomagnetic field including time dependence, radial diffusion and other details of radiation belt dynamics [5]. Predicted fluxes and spectral shapes of models differ from AP-8 NASA model noticeably. There is also large discrepancy in ³H/H ratio between model and experiments.

PAMELA has been acquiring data since July 11th 2006. The Resurs DK1 satellite orbit is elliptical and semi-polar, with an inclination of 70° and an altitude varying between 350 km and 610 km. The high performance instrument provides the separation of electrons, positrons, protons, antiprotons and light nuclei in wide energy range from 100 MeV up to several hundreds GeV [6]. Due to its orbit the PAMELA data-set covers the lower edge of the inner radiation belt in the South Atlantic Anomaly (SAA) region. This paper describes the instrument performance to observe trapped particles in SAA and preliminary results on composition of its fluxes.

II. INSTRUMENT

The PAMELA apparatus comprises the following sub-detectors: a time of flight system (ToF); a magnetic spectrometer; an anticoincidence system (AC); an electromagnetic imaging calorimeter; a shower tail catcher scintillator and a neutron detector. The ToF system provides a fast signal for triggering the data acquisition and measures the time-of-flight and ionization energy losses

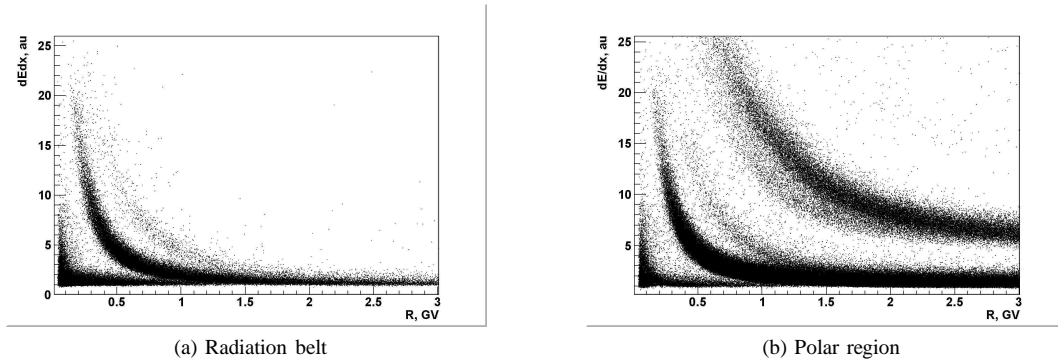


Fig. 1: dE/dx vs rigidity plots. Left panel is SAA, $B < 0.21G$, L -shell < 1.2 . From up to down lines of deuterium, protons, and positrons are visible. Right panel is polar region L -shell > 6 . In this region also He is presented.

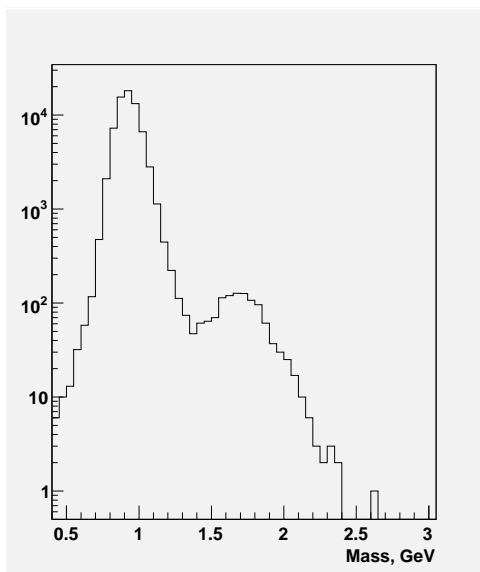


Fig. 2: Mass distribution for $Z=+1$ charge particles in SAA. $B < 0.21G$, $L < 1.2$.

of traversing particles. The central part of the PAMELA apparatus is a magnetic spectrometer consisting of a permanent magnet and a silicon tracking system. The spectrometer measures rigidities R of charged particles through their deflection in the magnetic field.

Particle identification is based on ionization energy losses dE/dx in ToF and spectrometer, determination of rigidity by the spectrometer, velocity β defined by time of flight and track length in the spectrometer and the properties of the energy deposit and interaction topology in the calorimeter.

Events with one hits in each of the ToF detectors and with only one track in the spectrometer were selected for analysis. Number of hits in spectrometer should be no less than 4 to provide good track fitting and consistent dE/dx value. Particle mass m can be reconstructed with equation (1) using R , charge Z and velocity β :

$$m = ZeR\sqrt{1/\beta^2 - 1} \quad (1)$$

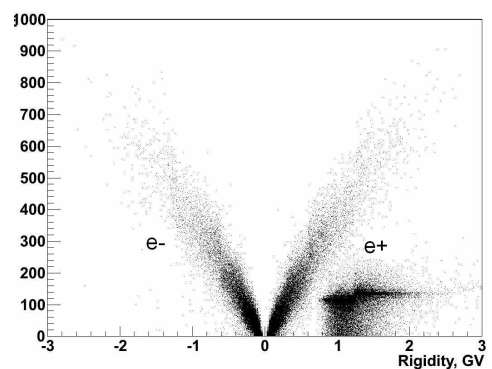


Fig. 3: Electron and positron discrimination in SAA $B < 0.21G$, $L < 1.2$.

Efficiencies of the track selection for protons, light nuclei were calculated by Monte-Carlo program based on GEANT-3 code. Orbital information such as an attitude, orientation and inclination of the satellite and PAMELA are determined on-board and recorded approximately once a second. It gives possibility to reconstruct pointing of the instrument with accuracy about $1-2^\circ$. Incoming angles of the particles into the instrument were calculated extrapolating fitted track in magnetic spectrometer to the upper ToF scintillator. Only particles with consistent ToF and spectrometer measurements were taken into account.

A geometric factor is $21\text{cm}^2\text{sr}$. Aperture is about 20 degrees.

To determine pitch-angle a position and an inclination of the satellite, ascending angles of incoming particles in the instrument are taken into account. Geomagnetic field was calculated using IGRF95 model.

More detail description of the instrument, orbit operations and data processing can be found in ref. [6]

III. OBSERVATIONS

SAA was selected with condition for geomagnetic field $B < 0.21G$. Only near equatorial region (L -shell < 1.2) was taken for analysis. The PAMELA instrument

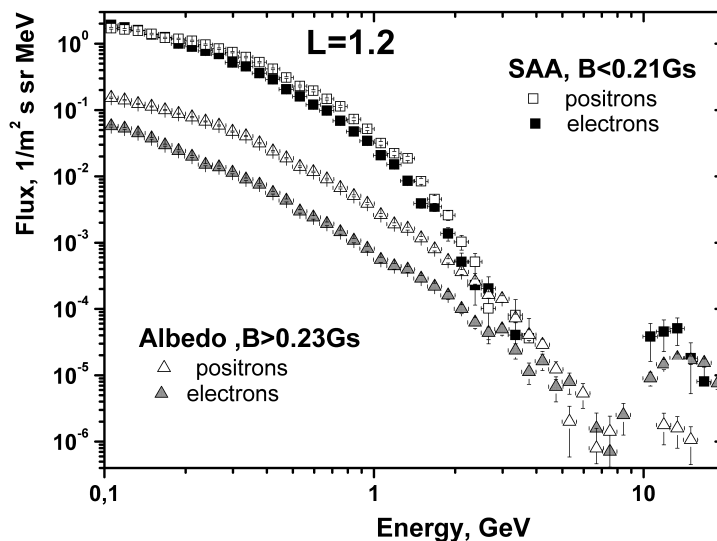


Fig. 4: Differential energy spectra of equatorial subcutoff (triangles) and trapped (squares) electrons (close points) and positrons (open points).

points to zenith except short intervals when the satellite makes a rotations. This orientation provides observation of particles with pitch-angles 70-130 degrees in the chosen region. It was shown [see M. Casolino, this conference] that proton flux is increasing significantly in this region. Trigger rate reaches 100 Hz in the core of region ($B < 0.19$ Gs) and it is close to the instrument limit. Meanwhile it is seen from the spectra that high energy ($E > 10$ GeV) it is not affected by high load of the instrument data acquisitions system. On this reason it is possible to rely on it that measurements at lower energies are also unbiased. Comparison of the spectra shows that inside SAA there is a fraction of high energy trapped particles with energy up to 2 GeV.

Figure 1 demonstrates dE/dx vs rigidity R plots for SAA region (left panel) and for polar region (right panel) where the instrument measure interplanetary cosmic rays. Even in condition of high background identification of hydrogen isotopes is possible by dE/dx measurements. Besides of good particle separation it is possible to see different composition of trapped particles. He nuclei are practically absent in SAA region at energy > 100 MeV/n.

Mass distribution of $Z=+1$ particles is shown on figure 2 for the rigidity interval $R=0.5-1.5$ GV. Distinct peak of deuterium is clearly seen on this figure. Some quantity of the secondary nuclei could be produced inside the instrument container in pA and HeA interactions. Thickness of the container is 2 mm of Al and if cross sections of those reactions are 30 mb and 100 mb accordingly an estimation based on known proton flux gives a contribution of ^2H background not more than 20-

30%. This estimation is consistent with observation of secondary deuterium production in the instrument during solar flare on 13 of December 2006. There were found about 10^2 ^2H nuclei candidates over 6000 protons at the same rigidity interval during one passage of polar region at the maximum of flare intensity when shape of proton spectra was similar to that observed in SAA. Because ^2H is absent in solar energetic particles the evidence of background production is clear. Normalization to proton flux gives 30% of background at energy 100-200 MeV/n. Last estimation can overestimate background because also He presented in solar particles in this time.

Figure 3 represents electron and positron discrimination capabilities in SAA using a topological variable as function of the rigidity. This variable takes into account the number of hits along the track in the calorimeter till an expected maximum of the electromagnetic shower. Hits are taken with weight that equal number of traversed planes. This variable tends to be smaller for non interacting protons or hadronic interacted particles [7]. Only particles with $\beta > 0.8$ were selected to plot this picture. Bands for electrons and positrons can be clearly distinguished. After applying full set of selection cuts contamination of protons becomes negligible in this region of space.

Differential energy spectra of trapped electrons and positrons are shown on figure 4. On this picture flux was averaged over all observed pitch-angles. Flux of trapped particles is several times more than albedo one in the equatorial region in agreement with previous measurements ([8] and references there). Like hydrogen isotopes additional electrons and positrons can be produced in

pA interactions of trapped protons with a residual atmosphere. The calculated e^+/e^- flux ratios in the belt due attain values of about 7 in the energy range of 10 to 300 MeV [9] that is in contradictions with our observations. At low energies (<100 MeV) also contribution of an acceleration mechanism is possible. It is seen from the figure 4 that charge ratio of trapped particles differs from albedo one and also varies with energy. Detail analysis of pitch-angle distribution of electron and positron fluxes is necessary to do to make a conclusion about the origin of additional lepton component in the inner radiation belt.

An estimation of trapped antiproton flux was made in energy range 200-400 MeV. Candidates were selected with negative rigidity, proper β and dE/dx . Then antiproton events can be clearly identified by annihilation star at the end of track in calorimeter. At present only upper limit 10^{-5} of $pbar/p$ ratio was determined because some of found events could be produced also in pA interactions inside the instrument. This flux is in an agreement with calculations in papers [10] and two order of magnitude higher an estimation done in paper [11].

IV. CONCLUSION

In spite of high intensity of particles in SAA, the PAMELA instrument keeps its characteristic to discriminate isotopes, electrons and positrons in this region. Composition and differential energy spectra of different species of trapped particles can be measured with high precision. By this PAMELA data can provide a new data for secondary radiation belt models.

V. ACKNOWLEDGMENTS

We acknowledge support from INFN, Italian Space Agency, Russian Federal Space Agency, Russian Base Research Foundation (grant 07-02-00922)

REFERENCES

- [1] Looper, M. D., J. B. Blake, J. R. Cummings, and R. A. Mewaldt, *SAMPEX observations of energetic hydrogen isotopes in the inner zone* Radiat.Meas.26,967-978,1996.
- [2] Bakaldin, A. Galper, S. Koldashov et al, *Geomagnetically trapped light isotopes observed with the detector NINA* JGR, v.107,A8,p1-8,2002
- [3] R. S. Selesnick and R. A. Mewaldt *Atmospheric production of radiation belt light isotopes*, v.101,A9,197451996
- [4] A.M. Galper, S. V. Koldashov, A. A. Leonov, and V. V. Mikhailov *Inner Radiation Belt Generation of Light Nuclei Isotope* Proc. 28thInt.CosmicRayConf.,4,42574260,Tsukuba,Japan,2003
- [5] R. S. Selesnick, M. D. Looper, and R. A. Mewaldt *A model of the secondary radiation belt* JGR,v.113,A11221,doi:10.1029/2008JA013593,2008
- [6] P. Picozza, A.M. Galper, G. Castellini et al., *PAMELA - A Payload for Antimatter Matter Exploration and Light-nuclei Astrophysics* Astropart.Phys.v.27,p.296-315,2007
- [7] E.Moccutti et al. *The PAMELA Electromagnetic Calorimeter: Flight Status* Proc.30thInt.CosmicRayConf.,Merida,Mexico, 2007
- [8] Galper, A. M., Dmitrenko, V. V., Gratchev, V. M. et al. *Electrons With Energy Exceeding 10 MeV in the Earth's Radiation Belt* RadiationBelts:ModelsandStandards. GeophysicalMonograph97.AGU.Washington,1996
- [9] A. Gusev,U.B. Jayanthi,G. Pugacheva et al. *Trapped positron flux formation in the innermost magnetosphere of the Earth* EarthPlanetsSpace,v.54,p.707-714,2002.
- [10] R. S. Selesnick, M. D. Looper, R. A. Mewaldt and A.W. Labrador *Geomagnetically trapped antiprotons* Geophys.Res. Lett.,v.34,L20104,doi:10.1029/2007GL031475,2007
- [11] G. Pugacheva,A. Gusev,U.B. Jayanthi et al. *Antiprotons confined in the earth inner magnetosphere* Astropart.Physics,v.20,p. 257-265,2003.